

Temperature dependence of critical currents in $\text{YBa}_2\text{Cu}_3\text{O}_{7-\delta}$ ceramics

Xiao-jun Yu and M. Sayer

Department of Physics, Queen's University, Kingston, Ontario, Canada K7L 3N6

(Received 29 October 1990; revised manuscript received 8 April 1991)

The temperature dependence of critical currents in $\text{YBa}_2\text{Cu}_3\text{O}_{7-\delta}$ superconducting ceramics have been studied following the Ginzburg-Landau theory and the de Gennes *proximity* effects for a superconductor-normal-conductor interface. Based on an $S/N/S$ weak-link model, critical currents as a function of temperature have been calculated and a model able to describe different kinds of I_c - T characteristics in 1:2:3 ceramics has been developed. A set of four $\text{YBa}_2\text{Cu}_3\text{O}_{7-\delta}$ ceramic samples has been prepared for experimental studies. These samples were annealed under different conditions. Critical currents as a function of temperature have been measured in a high-heat-transfer system. I_c - T characteristics ranging from a quadratic temperature dependence to a temperature dependence of the Josephson-tunneling type have been observed. The experimental I_c - T characteristics fit very well theoretical predictions which include the effects of randomness in the thickness of the nonsuperconducting barriers and the boundary conditions for the samples.

INTRODUCTION

Since the time when 90-K superconducting Y-Ba-Cu-O ceramics were discovered by Wu *et al.*,¹ many studies have focused on the critical currents in the high- T_c oxides. Experimental studies now have indicated that intergrain boundaries in the ceramic superconductors are a major factor limiting the critical current. As such, the intergrain boundaries are described as weak links.

Different types of weak links such as $S/I/S$ and $S/N/S$ may coexist in 1:2:3 ceramics, where S stands for superconductors, I for insulators between two superconductors, and N for normal conductors which are not superconductive at any temperatures or are superconducting with a lower transition temperature. However, it is generally agreed that $S/N/S$ weak links dominate in $\text{YBa}_2\text{Cu}_3\text{O}_{7-\delta}$ superconducting ceramics.^{2,3} A common practice to evaluate weak links is to study the temperature dependence of the critical current in the weak links.⁴ Many such studies have been made for 1:2:3 ceramics and different I_c - T characteristics varying from a linear to a quadratic temperature dependence at $T \rightarrow T_c$ have been reported by different authors.⁵⁻⁷ A comprehensive analysis of critical currents in $\text{YBa}_2\text{Cu}_3\text{O}_{7-\delta}$ films has been made by de Vries, Stollman, and Gijs *et al.*⁸ However, most reported I_c - T characteristics of 1:2:3 ceramics fall either into Clarke⁹ and Shih's¹⁰ models for classical $S/N/S$ weak links due to the de Gennes *proximity effect* or into the Ambegaokar and Baratoff (AB) model¹¹ for $S/I/S$ weak links due to Josephson tunneling. These wide discrepancies in the I_c - T characteristics are unlikely to be a result of error in experiments, and do reflect a variation in the properties of different samples even though $S/N/S$ weak links still dominate. As pointed out by Likharev¹² an $S/N/S$ weak link may exhibit an I_c - T characteristic of the Josephson tunneling type of the thickness of the normal layer is sufficiently thin. Deutscher and Müller¹³ predict that a transition from a

quadratic temperature dependence to a temperature dependence of the AB model is possible for weak links in 1:2:3 ceramic, but no detail is given for how this transition happens. Their prediction has been confirmed by our previous studies.³ So far, to our best knowledge, there is no single model which can describe such transitions in the I_c - T characteristics of $\text{YBa}_2\text{Cu}_3\text{O}_{7-\delta}$ ceramics.

In this paper, we report a model which is able to describe the I_c - T characteristics of $S/N/S$ weak links in $\text{YBa}_2\text{Cu}_3\text{O}_{7-\delta}$ ceramics. The model was developed following the Ginzburg-Landau theory and the de Gennes proximity effect. Experimental studies were performed by measuring critical currents in 1:2:3 ceramics as a function of temperature. A set of four samples have been prepared for the studies and their properties have been modified using different heat treatments. The effects of a thickness distribution of weak links on the I_c - T characteristics are discussed based on a Gaussian distribution.

THEORETICAL STUDIES

Based on the idea that a phase transition could be characterized by some kind of order parameter, Ginzburg and Landau (GL) introduced a complex, spatially varying wave function ψ as an order parameter for the superconducting electrons such that the local density of superconducting electrons was given by $n_s = |\psi|^2$. The theory is concerned with temperatures near T_c in which ψ is small, and it is postulated that ψ varies slowly in space. Based on these assumptions, the GL equations have been developed as

$$\alpha\psi + \beta|\psi|^2\psi - \frac{1}{2m^*} \left[\frac{\hbar}{i} \nabla - \frac{e^*}{c} \mathbf{A} \right]^2 \psi = 0, \quad (1)$$

$$\mathbf{J}_s = \frac{e^*\hbar}{i2m^*} (\psi^* \nabla \psi - \psi \nabla \psi^*) - \frac{e^{*2}}{m^*c} |\psi|^2 \mathbf{A}, \quad (2)$$

where m^* and e^* are the effective mass and electronic charge, respectively, \mathbf{A} the vector potential, α and β temperature-dependent coefficients, and \mathbf{J}_s is the supercurrent in a superconductor.

It has been proved that the GL equations are the limiting cases of the BCS microscopic theory at temperatures very close to T_c .¹⁴ This restriction guarantees that nonlocal superconductivity is not significant since the coherence length of a superconductor is much shorter than its magnetic penetration length at temperatures very close to T_c . For a *dirty* type-II superconductor, the electron mean free path is shorter than the coherence length ξ and ξ is in turn less than the magnetic penetration length. The restriction on temperatures for the validity of the GL equations can therefore be relaxed to some extent for *dirty* type-II superconductors. It has been reported that the GL equations hold approximately for a type-II superconductor over a temperature range from $0.7T_c$ to T_c .⁹ For $\text{YBa}_2\text{Cu}_3\text{O}_{7-\delta}$ ceramics, both l and ξ are very short. It is hard to define whether the materials are *dirty* or *clean* superconductors. Because local fluctuations dominate due to the very short coherence length, nonlocal superconductivity is not significant. Furthermore the magnetic penetration length λ of the superconductor is very long. A wider range of temperature for the GL equations to be applicable 1:2:3 ceramics is therefore expected.

When a normal conductor (N) is in good electrical contact with a superconductor (S), the Cooper pairs are able to diffuse into the normal conductor which then exhibits some superconducting properties. In addition, the presence of the normal conductor tends to lower the Cooper pair density in the vicinity of the S/N interface of the superconductor. This leads to a depressed order parameter in the superconductor and this phenomenon has become known as the *proximity effect*.

The depressed order parameter in the vicinity of the interface can be represented by a parametric function

$$f(x) = \frac{\psi(x)}{\psi_\infty}, \quad (3)$$

where ψ_∞ defines the order parameter deep inside the bulk superconductor. From this definition, $f(x)$ may vary between 0 and 1. In the absence of a magnetic field and current, the first GL equation [Eq. (1)] can be written as

$$\xi^2(T)f'' + f - f^3 = 0, \quad \xi^2(T) = \frac{\hbar^2}{2m^*|\alpha|}. \quad (4)$$

A solution can be obtained by integrating Eq. (4) partially such that

$$f(x, T) = \tanh \left[\frac{x + x_0}{\sqrt{2}\xi(T)} \right], \quad (5)$$

where x_0 is a parameter determined by the boundary conditions at the interface. If the normal layer is a magnetic material, $x_0 = 0$ since a magnetic material tends to destroy superconductivity. On the other hand, if the normal material is almost insulating x will be very large since an insulator imposed onto a superconductor will not significantly disturb the Cooper pair density in the super-

conductor. According to the second GL equation [Eq. (2)], a critical current can be calculated using the order parameter of a superconducting system.

In an $S/N/S$ weak link, two superconductors are separated by a nonsuperconducting layer N of thickness d . When d is not too large, the Cooper pairs can tunnel across the barrier. The effect of the nonsuperconducting layer is to impose boundary conditions relating the values of ψ and $(d\psi/dx)$ at one surface of N to the values at the other surface. If the thickness of N is small compared with the magnetic penetration length $\lambda(T)$ and the coherence length $\xi(T)$, the boundary conditions can be linearized as¹⁵

$$\psi_+ = M_{11}\psi_- + M_{12} \left[\frac{\partial\psi}{\partial x} \right]_-, \quad (6)$$

$$\left[\frac{\partial\psi}{\partial x} \right]_+ = M_{21}\psi_- + M_{22} \left[\frac{\partial\psi}{\partial x} \right]_-. \quad (7)$$

where the coefficients M_{ij} are real numbers and the subscripts $+$ and $-$ correspond to the two surfaces of the normal layer, respectively. In the presence of a small current, which is much less than the critical current in bulk superconductors, ψ can be slightly modified by introducing a phase parameter φ which is sensitive to currents and magnetic fields so that

$$\psi = \psi_0 e^{i\varphi}. \quad (8)$$

By substituting Eq. (6), (7), and (8) into Eq. (2), a supercurrent passing through an $S/N/S$ weak link is

$$J_s = \frac{2e\hbar}{m^*M_{12}} \psi_+ \psi_- \sin(\varphi_- - \varphi_+). \quad (9)$$

In deriving Eq. (9), the following relation required by the continuity of current has been used:

$$M_{11}M_{22} - M_{12}M_{21} = 1. \quad (10)$$

For two identical superconductors in an $S/N/S$ weak link, the maximum current density, i.e., critical current density, is thus given by

$$J_c = \frac{2e\hbar}{m^*M_{12}} \psi_b^2, \quad (11)$$

where ψ_b , which is defined by Eq. (3) and (5), is the order parameter at the surface of the bulk superconductor. The coefficient M_{12} depends on the transmission rate of the Cooper pairs from the superconductor to the normal layer, and the properties and the thickness of the nonsuperconducting layer. A detailed calculation by de Gennes¹⁶ shows that M_{12} is proportional to $\xi_N(T) \sinh[d/\xi_N(T)]$ so that the critical current can be written as

$$J_c = \frac{A}{\xi_N(T) \sinh(d/\xi_N(T))} \tanh^2 \left[\frac{x_0}{\sqrt{2}\xi_{\text{GLS}}(T)} \right] \psi_\infty^2(T), \quad (12)$$

where A is a constant of proportionality, ξ_{GLS} the GL coherence length, d the thickness of the nonsupercon-

ducting layer, and ξ_N the coherence length of the normal material. The coherence length has the form of $(hV_F l / 6\pi k_B T)^{1/2}$ if the mean free path l is less than the coherence length ξ_0 of the superconductor.

According to the GL theory, $|\psi|^2 \propto 1/\lambda^2$ and $\xi_{GLS} \propto 1/(H_c \lambda)$. The empirical temperature dependence of H_c and λ are $(1-t^2)$ and $(1-t^4)^{-1/2}$, respectively, where t is a reduced temperature T/T_c . The temperature dependence of the order parameter and the GL coherence length can thus be written

$$\psi_\infty \propto \sqrt{1-t^4} \quad \text{and} \quad \xi_{GLS} \propto \sqrt{(1+t^2)/(1-t^2)}. \quad (13)$$

At temperatures very close to T_c , $(1-t^4) \rightarrow 4(1-t)$ and $(1+t^2)/(1-t) \rightarrow 1$ the above equation reduces to

$$\psi \propto \sqrt{1-t} \quad \text{and} \quad \xi_{GLS} \propto \sqrt{1/(1-t)}. \quad (14)$$

The term $[1 - \exp(-2d/\xi_N)]$ in $\sinh(d/\xi_N)$ is not as sensitive as ψ_∞ and ξ_{GLS} , and the term $\tanh(x_0/\xi_{GLS}) \rightarrow x_0/\xi_{GLS}$ in Eq. (12). Thus Eq. (12) reduces to Shih's model

$$I_c \propto \left[1 - \frac{T}{T_c} \right]^2 \exp \left[-\frac{d}{\xi_N(T)} \right]. \quad (15)$$

A quadratic temperature dependence is therefore expected at temperatures close to T_c . Since we intend to apply the GL equations to lower temperatures, Eq. (13) must be used instead of Eq. (14), for calculations of critical currents as a function of temperature. At temperatures not very close to T_c but still high enough for the GL equations to be valid, the I_c - T characteristics of 1:2:3 ceramics are determined by two parameters: the thickness d of the normal layer and the value of order parameter at the grain surface determined by x_0 . Figure 1 shows I_c - T curves for different d values with a constant x_0 , calculated according to Eq. (12), and Fig. 2 shows the curves for different x_0 values with a constant d . It is clear that

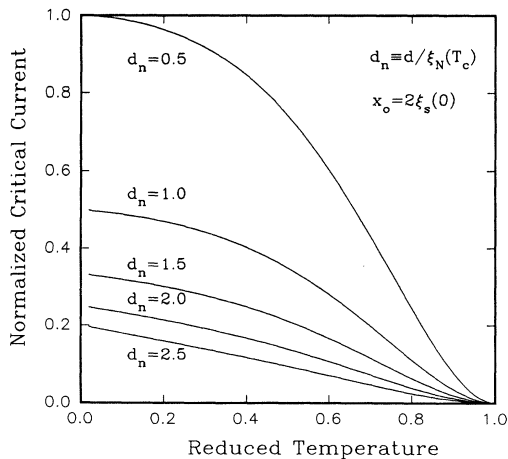


FIG. 1. Normalized critical currents vs temperature for different d values with a constant x_0 .

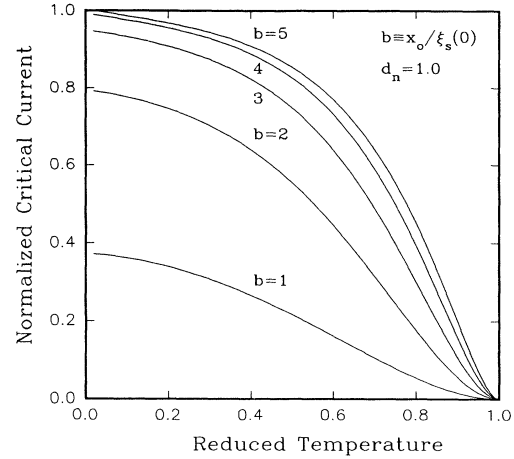


FIG. 2. Normalized critical currents vs temperature for different x_0 values with a constant d of 2.

an $S/N/S$ weak link can exhibit different I_c - T characteristics. The wide discrepancies in the reported temperature dependence of critical currents can thus be explained by this model.

EXPERIMENTAL STUDIES

A set of four samples were prepared for measurements of the critical current as a function of temperature. Samples of size $2 \times 0.3 \times 15 \text{ mm}^3$ were cut from a single bar of $\text{YBa}_2\text{Cu}_3\text{O}_{7-\delta}$ which was sintered at 935°C in air with a cooling rate of $1^\circ\text{C}/\text{min}$. The samples were then subjected to different heat treatments. One sample was left as prepared and the other three samples were annealed in oxygen at temperatures of 400°C , 750°C , and 900°C for different periods of time, respectively, as listed in Table I. All samples were cooled to room temperature at a rate of $1^\circ\text{C}/\text{min}$. Electrodes were made by thermal deposition of silver across the sample in a four-probe pattern. The leads were soldered to the silver with indium using an ultrasonic soldering iron.

Weak links in $\text{YBa}_2\text{Cu}_3\text{O}_{7-\delta}$ ceramics were studied experimentally by measuring the critical currents as a function of temperature. Unlike traditional superconductors, most of which are pure metals, $\text{YBa}_2\text{Cu}_3\text{O}_{7-\delta}$ is a ceramic compound. It is difficult to make low-resistance contacts as electrodes. The contact resistance of electrodes is always significant and causes Joule heating at the electrodes when the applied currents are high. This effect is called a *self-heating effect*. It has been found that a

TABLE I. Oxygen annealing conditions of the samples.

Sample	Temperature ($^\circ\text{C}$)	Time (h)	T_c (K)
1	None	None	90.2(2)
2	400	0.5	91.3(2)
3	750	30	91.5(2)
4	900	3	91.3(2)

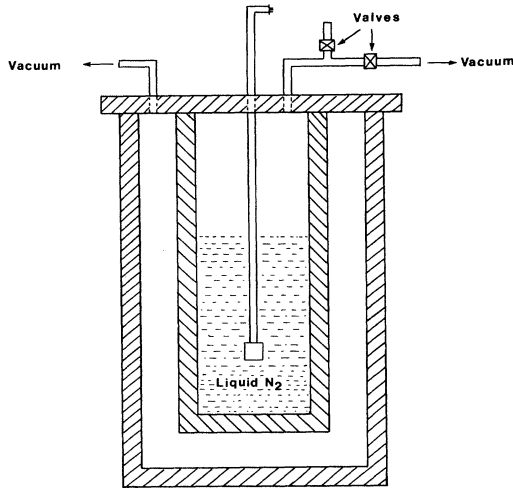


FIG. 3. A diagram of the cryostat for measurements of critical currents as a function of temperature.

current as small as 100 mA can produce sufficient heat to warm up the sample and thus cause an unstable temperature measurement. A key factor in accurate measurements of critical currents in ceramic superconductors as a function of temperature is to eliminate the self-heating effect.

It has been reported that the contact resistance can be reduced significantly by annealing the silver electrode pads in oxygen.¹⁷ This technique was found, however, not to be applicable to this work because the I_c - T characteristics of a nonannealed sample were compared with those of annealed samples. As it will be noted later, the I_c - T characteristics can be changed significantly after annealing at 400 °C over a period of time as short as 30 min. Furthermore, one sample was annealed at a temperature of 900 °C, which was much higher than that (500–600 °C) at which silver pads are normally annealed.^{18,19} The wide range of annealing temperatures used would therefore make it difficult to obtain reproducible contact electrodes for all samples.

The self-heating effect was minimized by immersing a sample in liquid nitrogen during measurements. Heat produced at the electrodes was carried away quickly by liquid nitrogen. The sample temperature was controlled by varying the pressure above the liquid. Figure 3 shows a diagram of the cryostat designed for measurements of critical currents as a function of temperature. The chamber was sealed during measurements so that a negative or a positive pressure, controlled by two pressure re-

TABLE II. Results of XRD analysis of the annealed samples.

Sample	a (Å)	b (Å)	c (Å)	Volume (Å ³)
1	3.824(1)	3.890(1)	11.680(5)	173.75(16)
2	3.820(1)	3.888(1)	11.672(4)	173.41(15)
3	3.821(1)	3.887(1)	11.671(5)	173.34(16)
4	3.822(1)	3.887(1)	11.672(4)	173.41(15)

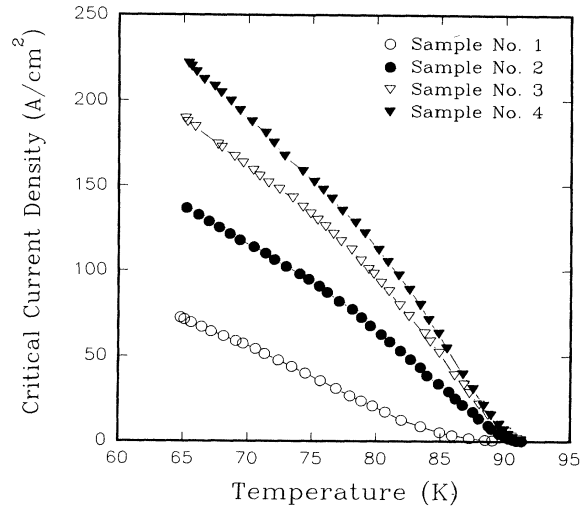


FIG. 4. Experimental J_c - T characteristics of the four samples. Curve No. 1 is for a sample as prepared. Curve No. 2 is for a sample annealed at 400 °C in oxygen for 0.5 h. Curve No. 3 is for a sample annealed at 750 °C in oxygen for 30 h. Curve No. 4 is for a sample annealed at 900 °C in oxygen for 5 h.

gulators, could be obtained by either lowering or increasing the pressure. To facilitate increasing the pressure, a small resistance heater was used to boil the liquid nitrogen. By this method, self-heating effects were eliminated and the sample temperature was maintained constant over a range 64–95 K. The temperature was measured with an uncertainty of ± 0.2 K using a copper-constant thermocouple which was attached to the sample.

The critical currents in the samples were measured by

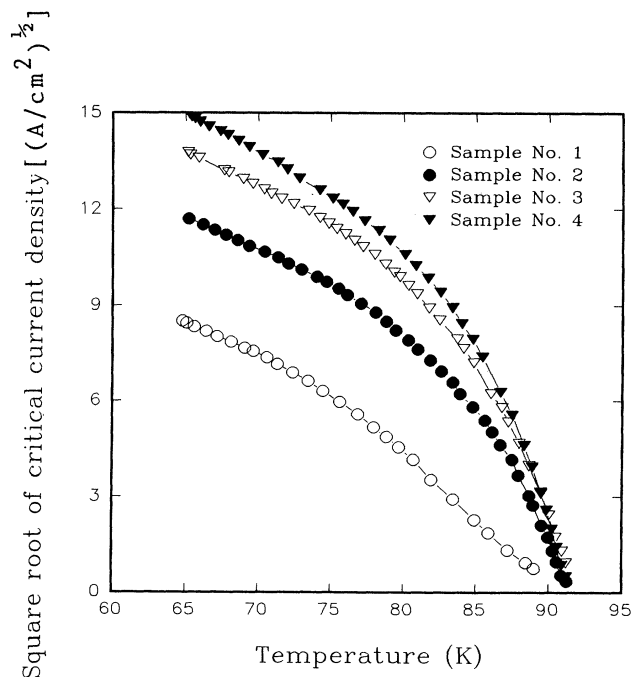


FIG. 5. Replot of Fig. 4 in a manner of the square root of the critical current densities vs temperatures.

a four-probe method. The voltage criterion to define J_c is $0.1 \mu\text{V}$ for a distance of 3.3 mm between two electrodes. This is equivalent to an electric field of $3 \times 10^{-7} \text{ V/cm}$. The critical current densities were obtained by dividing the measured critical currents by the cross sectional area of the sample. The transition temperature was defined as the temperature for which the critical current density J_c was 0.2 A/cm^2 .

The effect of the technique for elimination of the self-heating effects has been checked by measuring the critical current in a sample of which the silver electrode pads were annealed in oxygen at 500°C for 1 h. No significant difference in J_c - T characteristics was observed compared with samples of which the silver electrode pads were not annealed.

RESULTS AND DISCUSSIONS

The lattice constants of the samples were measured by x-ray diffraction (XRD). Results are summarized in Table II. All the samples are single phase $\text{YBa}_2\text{Cu}_3\text{O}_{7-\delta}$ within the uncertainty (2–3 %) of the instrument. The volume of the unit cell of the sample with no post oxygen annealing is clearly the largest for all samples. The unit cell for samples annealed in oxygen did not change within experimental uncertainty.

Different kinds of temperature dependence of critical current in the samples have been observed. As shown in Fig. 4, the J_c - T characteristic of the sample with no oxygen annealing is quadratic over the most of the range of measured temperature. This quadratic temperature

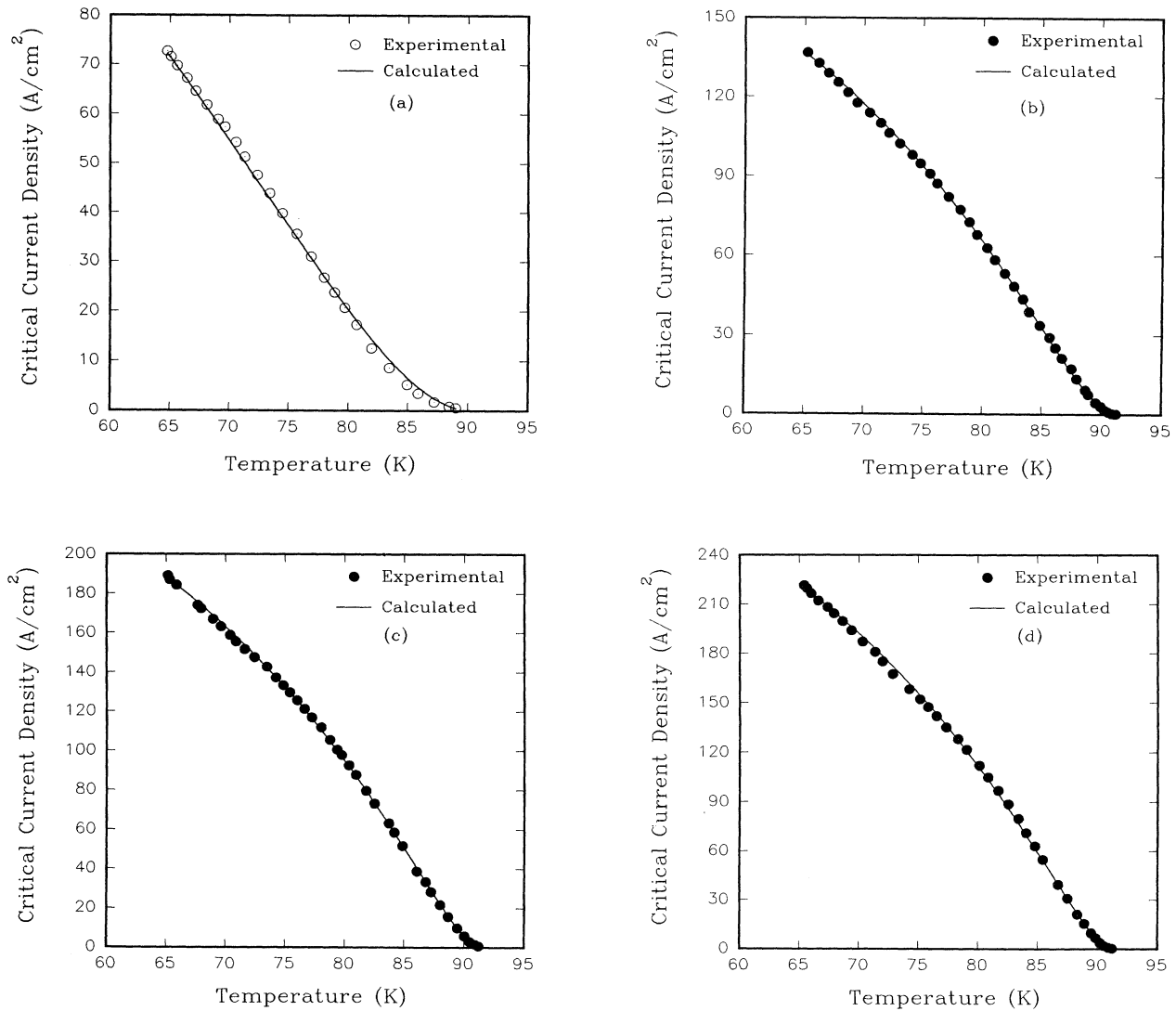


FIG. 6. (a) Fitted J_c to sample No. 1 according to Eq. (12), using parameters $A=490$, $d/\xi_N(T_c)=1.4$ and $x_0/\xi_{\text{GLS}}(0)=2.15$. (b) Fitted J_c to sample No. 2 according to Eq. (12), using parameters $A=621$, $d/\xi_N(T_c)=1.35$ and $x_0/\xi_{\text{GLS}}(0)=4.85$. (c) Fitted J_c to sample No. 3 according to Eq. (12), using parameters $A=745$, $d/\xi_N(T_c)=1.23$ and $x_0/\xi_{\text{GLS}}(0)=5.5$. (d) Fitted J_c to sample No. 4 according to Eq. (12), using parameters $A=850$, $d/\xi_N(T_c)=1.2$ and $x_0/\xi_{\text{GLS}}(0)=5.75$.

TABLE III. Fitting parameters for J_c of the samples.

Sample	$A/\xi_N(T_c)$	$x_0/\xi_{GLS}(0)$	$d/\xi_N(T_c)$
1	490	2.15	1.40
2	621	4.85	1.35
3	745	5.50	1.23
4	850	5.75	1.20

dependence also holds at temperatures close to T_c for all samples. As the annealing temperature increases, the quadratic behavior disappears. This property can be seen clearly in Fig. 5 where $J_c^{1/2}$ is plotted versus temperature for the samples.

Calculated critical current densities according to Eq. (12) are compared with experimental results. As shown in Fig. 6, the J_c - T characteristics of all samples except for sample No. 1 can fit very well to the model. The J_c - T characteristic of sample No. 1 shows a power relation. The discrepancy is likely due to a wide distribution of thickness of the weak links and this effect will be discussed later. The fitting parameters are listed in Table III.

As we have proposed previously, oxygen annealing mainly affects the surfaces of crystal grains.³ The oxygen content at the surface of the crystal grains increases after annealing. During annealing, oxygen enters into the grain surface of ceramic samples very quickly even at low temperatures.²⁰ The enhancement of oxygen in the superconductor will result in an increase in carrier density and in the order parameter at the edge of the crystal grains.³ A large order parameter is favorable to both Josephson tunneling¹² and high critical current density. These arguments can now be supported by the excellent agreement between the experimental and the calculated results. As indicated in Table III, the reduction of the barrier width is almost constant for the four samples. The x_0 values, however, increase significantly from sample No. 1 to sample No. 3. For these the J_c - T characteristics change quite noticeably. The x_0 values determine the order parameter at the edge of the S/N interface in Eq. (6), and the larger the x_0 the higher is the order parameter for tunneling.

In Fig. 6, the calculated J_c - T curve does not agree well with results for sample No. 1, which was not annealed in oxygen. We believe that the discrepancy is likely due to randomness within the sample. Different weak links could coexist in the ceramic samples. The critical current and its temperature dependence will be determined by the properties of the weak links which predominate in the sample. Equation (12) is derived based on a single $S/N/S$ weak-link model. If a sample is homogeneous, most weak links in the sample have similar properties and a single weak-link model can work well. On the other hand, a discrepancy between the model and the experimental results is expected if a sample is not homogeneous. The homogeneity of the sample can be illustrated by examining its I - V characteristic. As shown in Fig. 7(a) and 7(b), the I - V curve for a sample sintered

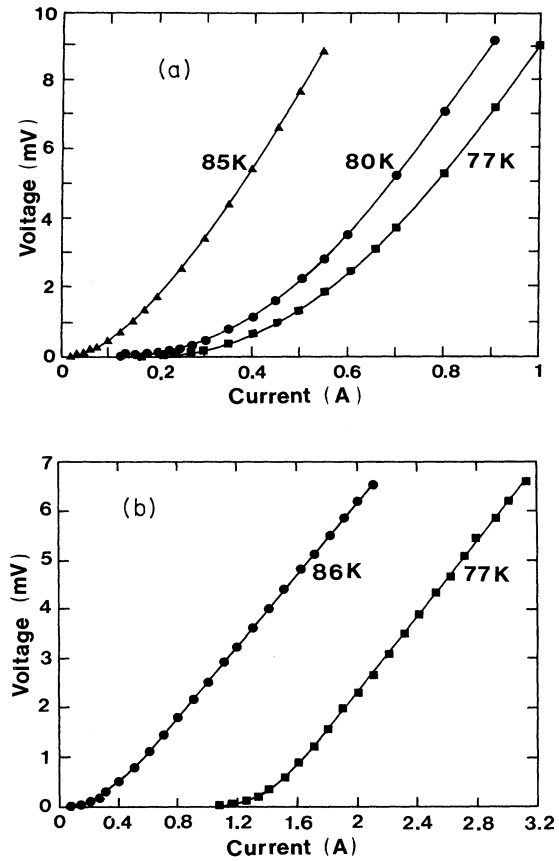


FIG. 7. I - V characteristics of $\text{YBa}_2\text{Cu}_3\text{O}_{7-\delta}$ samples sintered in air (a) and sintered in oxygen (b).

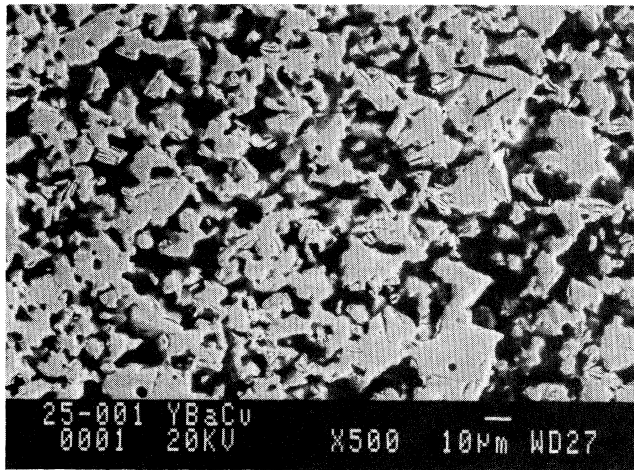
in air is less linear at applied currents in excess of I_c than that for a sample sintered in oxygen, which has similar properties as those for a sample annealed at 900 °C in oxygen. Although the authors have not attempted to calculate such I - V characteristics of the samples using the $S/N/S$ junction model, Blair has shown that the linearity of the I - V curves of $\text{YBa}_2\text{Cu}_3\text{O}_{7-\delta}$ reflects the homogeneity of the materials²¹ using a one-dimensional percolation model for the ceramics. According to Fig. 7, the sample sintered in air with no post annealing is not as homogeneous as those annealed in oxygen. This argument can be further supported by scanning electron microscopy (SEM) of the samples. As shown in Fig. 8(a) and 8(b), impurities such as copper-rich materials have been found to be segregated at grain boundaries of the samples which were not annealed in oxygen and were annealed at low temperatures for a short period of time. No such impurities were found in samples annealed at higher temperatures as shown in Fig. 8(c) and 8(d). Large chunks of crystal grains were found in the sample sintered at 900 °C. These results indicate that the homogeneity of a ceramic sample can be improved after oxygen annealing.

We can estimate the effects of a distribution in thickness d and boundary condition x_0 by arbitrarily employing a Gaussian distribution for these two parameters:

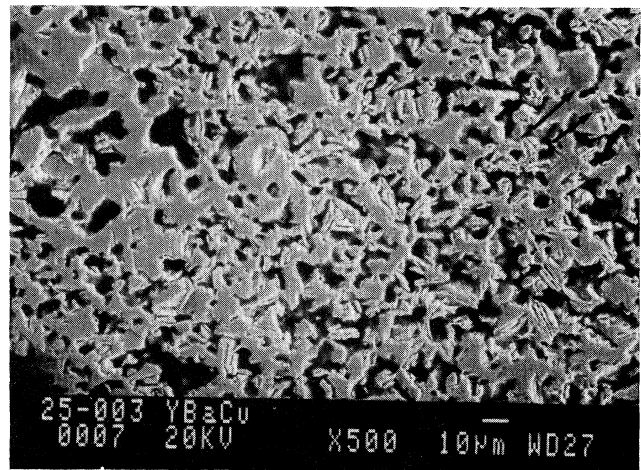
$$J_c = A' \psi_\infty^2(T) \sum_{i=1}^{N_i} \sum_{j=1}^{N_j} \frac{\tanh^2 \left[\frac{j\Delta x}{\sqrt{2}\xi_{\text{GLS}}(T)} \right] \exp \left[- \left(\frac{i\Delta d - d_0}{w_d} \right)^2 \right] \exp \left[- \left(\frac{j\Delta x - x_0}{w_x} \right)^2 \right]}{\xi_N(T) \sinh \left[\frac{i\Delta d}{\xi_N(T)} \right]}, \quad (16)$$

where Δx and Δd are increments, and w_x and w_d are half-height widths of x_0 and d_0 , respectively. By introducing $w_d=4$, $w_x=1$, with d_0 and x_0 the same values as those in Table III for sample No. 1, the agreement between the calculated $J_c(T)$ and experimental values of sample No. 1, especially at temperatures close to T_c , has

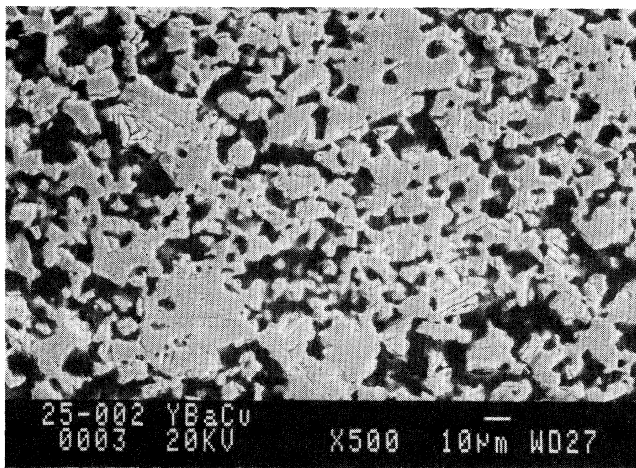
been improved as shown in Fig. 9. However, it is noted that this result is only a guideline to consider how randomness within a sample could influence the I_c - T characteristics. No conclusions can be drawn about the distribution of thickness in a set of nonsuperconducting barriers without further studies of the sample properties.



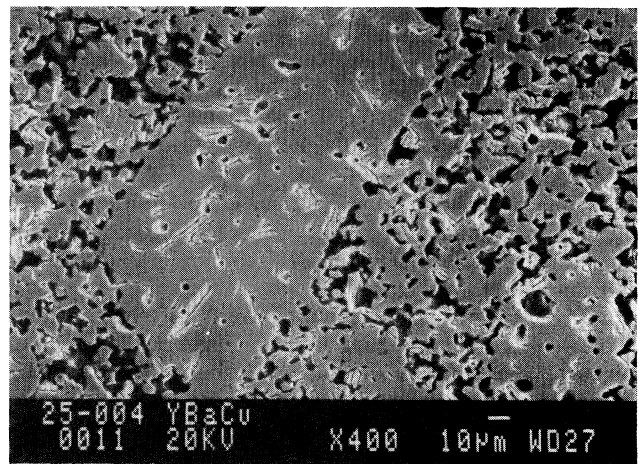
(a)



(b)



(c)



(d)

FIG. 8. SEM pictures for the annealed samples. (a) The microstructure of the as-prepared sample. (b) The microstructure of the sample annealed at 400°C. (c) The microstructure of the sample annealed at 750°C. (d) The microstructure of the sample annealed at 900°C.

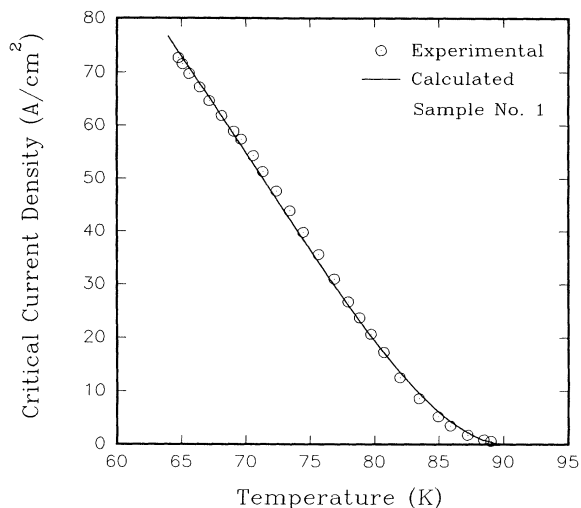


FIG. 9. Fitted J_c of sample No. 1 using Eq. (16).

Finally we would like to point out that the validity of Eq. (13) depends on whether the empirical temperature dependence of H_c and λ determined for traditional low-temperature superconductors, which are described well by the BCS theory, are applicable to $\text{YBa}_2\text{Cu}_3\text{O}_{7-\delta}$ superconductors. It has been found that the temperature dependence of the magnetic penetration depth λ of $\text{YBa}_2\text{Cu}_3\text{O}_{7-\delta}$ can be well described by the empirical temperature dependency we have used.^{22,23} Our studies of the specific heat of $\text{YBa}_2\text{Cu}_3\text{O}_{7-\delta}$ ceramics have shown that $H_c(T)$ varies with temperature in a manner de-

scribed by $H_c(T) \propto (1-t^n)$ with $n = 1.8 \pm 0.2$.²⁴ This is, in fact, very close to the expected value of 2 after taking the errors of experiments and calculations into account. These results imply that the $\text{YBa}_2\text{Cu}_3\text{O}_{7-\delta}$ superconductors can be described by the BCS theory.

CONCLUSIONS

The temperature dependence of critical currents in $\text{YBa}_2\text{Cu}_3\text{O}_{7-\delta}$ ceramics have been studied theoretically following the Ginzburg-Landau theory. Based on an $S/N/S$ weak-link model, a model for the I_c - T characteristics of 1:2:3 ceramics has been developed which describes different kinds of temperature dependence for the critical current in a ceramic sample. By measuring critical currents as a function of temperature in samples subjected to different annealing conditions, different I_c - T characteristics, from a quadratic temperature dependence to a temperature dependence of the Josephson-tunneling type, have been observed. Good agreement between calculated critical currents and measured critical currents at different temperatures has been achieved. Both theoretical and experimental studies indicate that oxygen annealing of ceramic samples mainly affects the surface of the superconducting grains and that randomness in a sample influences its I_c - T characteristics.

ACKNOWLEDGMENTS

We would like to thank Dr. R. D. Heiding for the XRD analysis of the samples and Mrs. L. Devlin for SEM pictures. This work was supported by the Natural Sciences and Engineering Research Council of Canada.

¹M. K. Wu, J. R. Ashburn, C. J. Torng, P. H. Hor, R. L. Meng, L. Gao, Z. J. Huang, Y. Q. Wang, and C. W. Chu, *Phys. Rev. Lett.* **58**, 908 (1987).

²J. Mannhart, P. Chaudhari, D. Dimos, C. C. Tsuei, and T. R. McGuire, *Phys. Rev. Lett.* **61**, 2476 (1988).

³X. Yu and M. Sayer, *Physica C* **159**, 496 (1989).

⁴H. C. Yang and H. E. Horng, *J. Low Temp. Phys.* **70**, 493 (1988).

⁵J. Aponte, H. C. Abache, A. Sa-Neto, and M. Octavio, *Phys. Rev. B* **39**, 2233 (1989).

⁶S. S. Yom, T. S. Hahn, Y. H. Kim, H. Chu, and S. S. Choi, *Appl. Phys. Lett.* **54**, 2370 (1989).

⁷J. W. C. de Vries, M. A. M. Gijs, G. M. Stollman, T. S. Baller, and G. N. A. van Veen, *J. Appl. Phys.* **64**, 426 (1988).

⁸J. W. C. de Vries, G. M. Stollman, and M. A. M. Gijs, *Physica C* **157**, 406 (1989).

⁹J. Clarke, *Proc. R. Soc. London, Ser. A* **308**, 447 (1969).

¹⁰W. Y. Shih, C. Ebner, and D. Stroud, *Phys. Rev. B* **30**, 134 (1984).

¹¹V. Ambegaokar and A. Baratoff, *Phys. Rev. Lett.* **10**, 468 (1963).

¹²K. K. Likharev, *Rev. Mod. Phys.* **51**, 101 (1979).

¹³G. Deutscher and K. A. Müller, *Phys. Rev. Lett.* **59**, 1754

(1987).

¹⁴L. P. Gor'kov, *Zh. Eksp. Teor. Fiz.* **36**, 1918 (1959) [*Soviet Phys. JETP* **9**, 1364 (1959)].

¹⁵P. G. de Gennes, *Superconductivity of Metal and Alloys* (Benjamin, New York, 1966).

¹⁶P. G. de Gennes, *Rev. Mod. Phys.* **36**, 225 (1964).

¹⁷J. Ekin, A. J. Panson, and B. A. Blankenship, *Appl. Phys. Lett.* **52**, 531 (1988).

¹⁸J. Ekin, T. M. Larson, N. F. Bergren, A. J. Nelson, A. B. Swartzlander, L. L. Kazmerski, A. J. Panson, and B. A. Blankenship, *Appl. Phys. Lett.* **52**, 1819 (1988).

¹⁹Y. Tzeng, A. Holt, and R. Ely, *Appl. Phys. Lett.* **52**, 155 (1988).

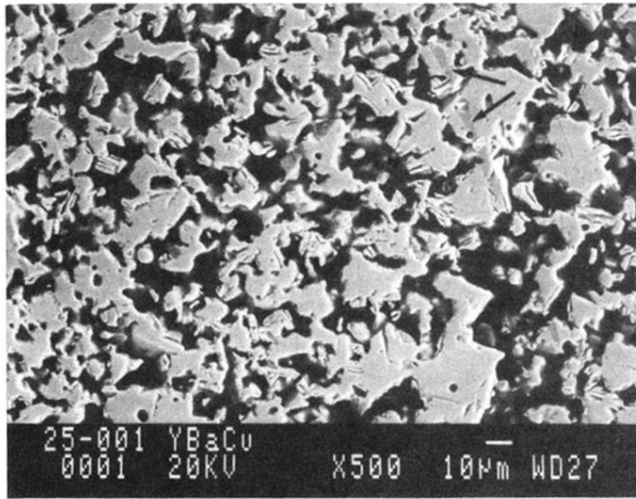
²⁰K. N. Tu, N. C. Yeh, S. I. Park, and C. C. Tsui, *Phys. Rev. B* **39**, 304 (1989).

²¹M. G. Blamire (unpublished).

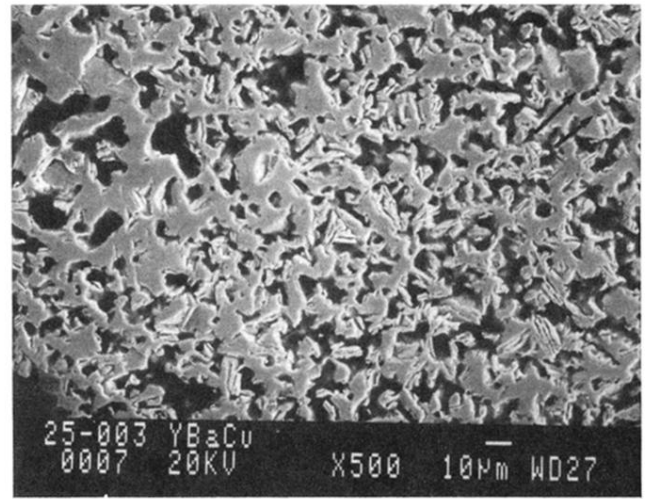
²²D. R. Harshman, G. Aeppli, E. K. Ansaldo, B. Batlogg, J. H. Brewer, J. F. Carolan, R. J. Cava, and M. Celio, *Phys. Rev. B* **36**, 2386 (1987).

²³Dong-Ho Wu and S. Sridhar, *Phys. Rev. Lett.* **65**, 2074 (1990).

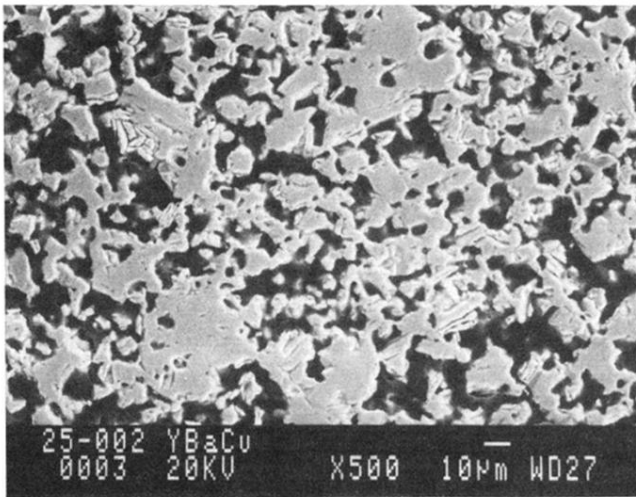
²⁴X. Yu, Ph.D thesis, Queen's University at Kingston, Ontario, Canada, 1991 (unpublished).



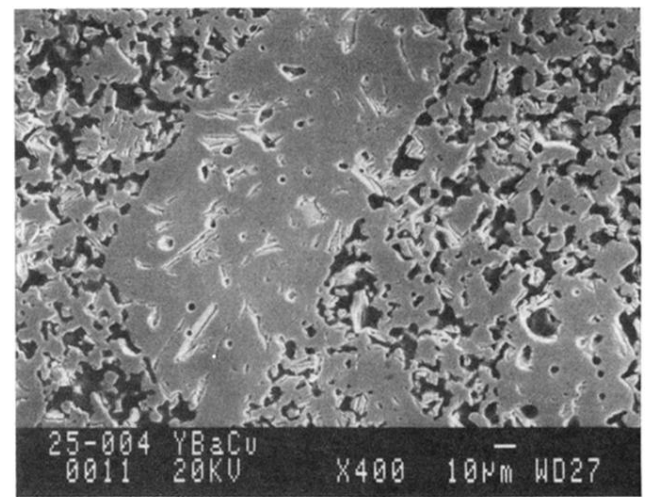
(a)



(b)



(c)



(d)

FIG. 8. SEM pictures for the annealed samples. (a) The microstructure of the as-prepared sample. (b) The microstructure of the sample annealed at 400°C. (c) The microstructure of the sample annealed at 750°C. (d) The microstructure of the sample annealed at 900°C.